

Supporting information

Size-dependent Magnetic Properties of NiO Nanoparticles Synthetized via Ni-hydroxy-acetate Decomposition

Miran Baričić,^{a,b*} Pierfrancesco Maltoni^{b,c}, Giulia Franceschin^{a,d}, Thomas Gaudisson^a, Sophie Nowak^a, Frederic Mazaleyrat^d, Davide Peddis^{b,c}, Souad Ammar^{a*}.

¹ Université Paris Cité, CNRS, ITODYS (UMR-7086), Paris 75205 Paris, France

² University of Genoa, Department of Chemistry and Industrial Chemistry & INSTM RU, nM2-Lab, Genova 14146, Italy

³ National Research Council (CNR), Institute of Structure of Matter (ISM), nM2-Lab, Roma 00015, Italy

⁴ Université Paris-Saclay, ENS Paris-Saclay, CNRS, SATIE (UMR- 8029), Gif-sur-Yvette 91190, France

Ni-LHS structure

The shift at higher angles of the (00l) peaks of the LHS can be attributed to the loss of water and acetate molecules in then interlayer space, making the basal space shrink. The inter-layer space obtained for the pristine Ni-LHS is very similar to that of the polyol made Ni-LHS produced by Poul *et al.*[1] (10,5 Å), while the interplanar distances relative to the (100) and (110) intra-layer reflections are very similar to those obtained for the peaks with same Miller indexes of β -Ni(OH)₂[2] (2,71 Å and 1,56 Å), confirming our structural interpretation.

Table S1: (001) peak position (2θ) and interplanar spacing ($d_{(001)}$) features of the LHS phases obtained in the annealing process

T (°C)	$2\theta_{(001)}$ (°)	$d_{(001)}$ (Å)	$2\theta_{(100)}$ (°)	$d_{(100)}$ (Å)	$2\theta_{(110)}$ (°)	$d_{(110)}$ (Å)
Pristine	9.46	10.8	39.00	2.68	70.44	1.55
220	11.62	8.8	39.12	2.67	70.60	1.55
240	12.49	8.3	39.15	2.68	70.74	1.55

Transmission Electron Micrographs recorded after different annealing temperatures of Ni-LHS

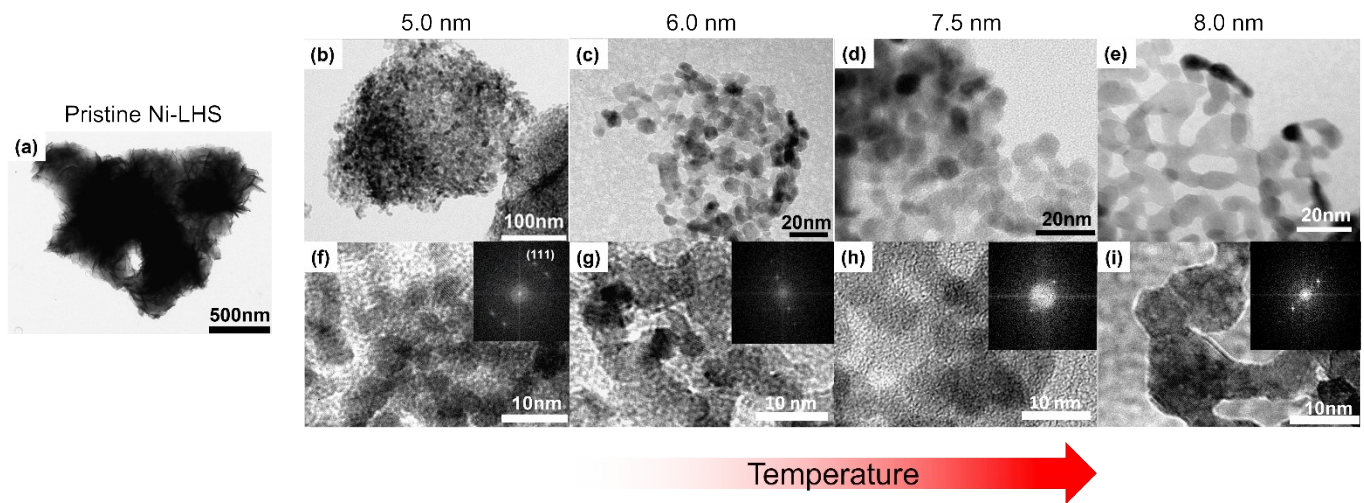


Figure S1: TEM images of a selection of samples. Image a) shows the pristine Ni-LHS, while images b), c), d) and e) show the pictures of NiO obtained after 2 h at 300, 360, 420, and 460°C. Images f), g), h) and i) show higher magnification TEM pictures of the same NiO samples, with FFT in the inset.

Magnetic properties of Ni-LHS

Isothermal $M(H)$ curves are measured for the pristine and the 240°C treated Ni-LHS phases. Layered hydroxides and hydroxy acetates are ferromagnetic materials with relatively high saturation magnetizations. Although their critical temperature is usually in the order of 10-20 K, very small LHS impurities can confuse the interpretation of magnetic data, when studying antiferromagnets, which generally have much lower magnetizations respect to ferromagnets. However, the decomposition of the LHS phase is observed in TGA curves at ~300°C, and no signs of the magnetic properties of the LHS can be observed in the measurements of NiO sample.

Table S2: coercivity ($\mu_0 H_c$), saturation magnetization (M_s), remanent magnetization (M_r), and squareness ratio (or reduced remanence, m_r) of the pristine and the treated layered hydroxides.

Sample	$\mu_0 H_c$ (mT)	M_s (Am ² kg ⁻¹)	M_r (Am ² kg ⁻¹)	m_r (a.u.)
Pristine	77	87	38	0.44
240°C	65	82	25	0.30

NiO Crystal size and crystal unit cell parameter

Table S3: annealing temperature, crystal size and lattice parameter of the selection of samples on which magnetic properties were measured.

Sample	$T_{\text{annealing}}$	d_{XRD}	a (Å)
--------	------------------------	------------------	---------

	(°C)	(nm)	
NiO_4.5	260	4.5(5)	4.189(2)
NiO_5.0	300	5.0(5)	4.184(2)
NiO_5.5	340	5.5(5)	4.182(2)
NiO_6.0	360	6.0(5)	4.184(2)
NiO_7.5	420	7.5(5)	4.180(2)
NiO_10.5	500	10.5(5)	4.176(2)
NiO_14.0	540	14.0(5)	4.176(2)
NiO_18.0	600	18.0(5)	4.176(2)

Magnetic properties of NiO

As already explained in the main text, the AFM hysteresis loops are analyzed as a sum of a Fm-like contribution and a high-field (HF) linear susceptibility term, and can be expressed as $M(H) = M_{FM}(H) + \chi_{HF}H$, in accordance with what is already presence in literature[3]. A schematic representation of the operation is provided in **Figure S2**.

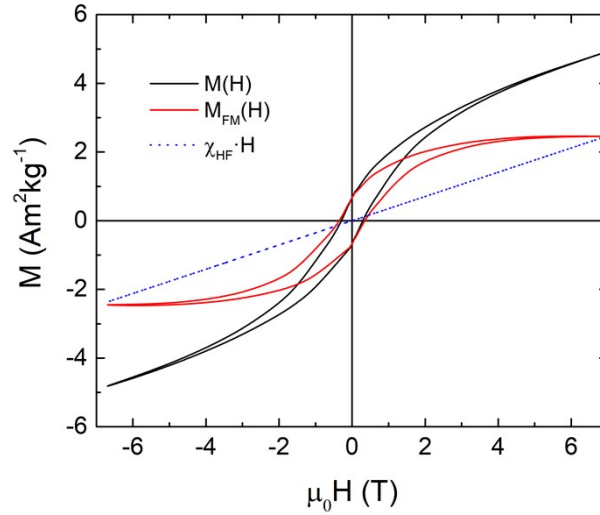


Figure S2: experimental hysteresis of NiO (black), FM-like component (red), and high field susceptibility linear dependence (dashed blue).

Table S4: ZFC and FC coercivities (μ_0H_c ZFC and FC), exchange bias (μ_0H_{EB}), ferromagnetic magnetization (M_{sFM}), and ZFC/FC remanence of the series of NiO samples. Error on the last digit in parentheses.

Sample	μ_0H_c (ZFC) (mT)	μ_0H_c (FC) (mT)	μ_0H_{EB} (mT)	M_{sFM} (Am²kg⁻¹)	M_r (ZFC) (Am²kg⁻¹)	M_r (FC) (Am²kg⁻¹)
NiO_4.5	288	342	76	2.46	0.672	0.924
NiO_5.0	352	492	221	1.20	0.354	0.706
NiO_5.5	327	478	239	0.638	0.172	0.387
NiO_6.0	422	611	263	0.452	0.157	0.308
NiO_7.5	314	631	817	0.338	0.105	0.415
NiO_10.5	237	595	1262	0.0876	0.0480	0.281
NiO_14.0	211	575	844	0.111	0.0224	0.248
NiO_18.0	60.2	85.7	174	0.270	0.0180	0.0909

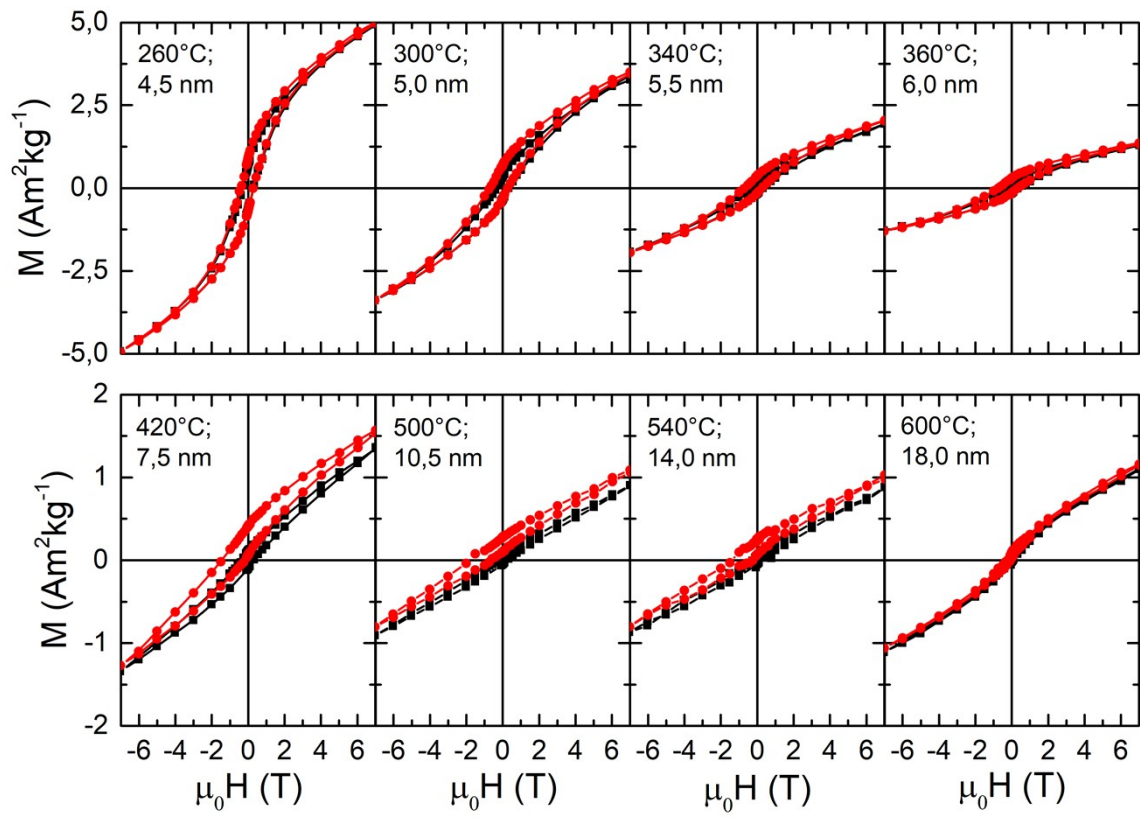


Figure S3: 5 K $M(H)$ loops of the NiO samples in ZFC (black) and FC (red) modes.

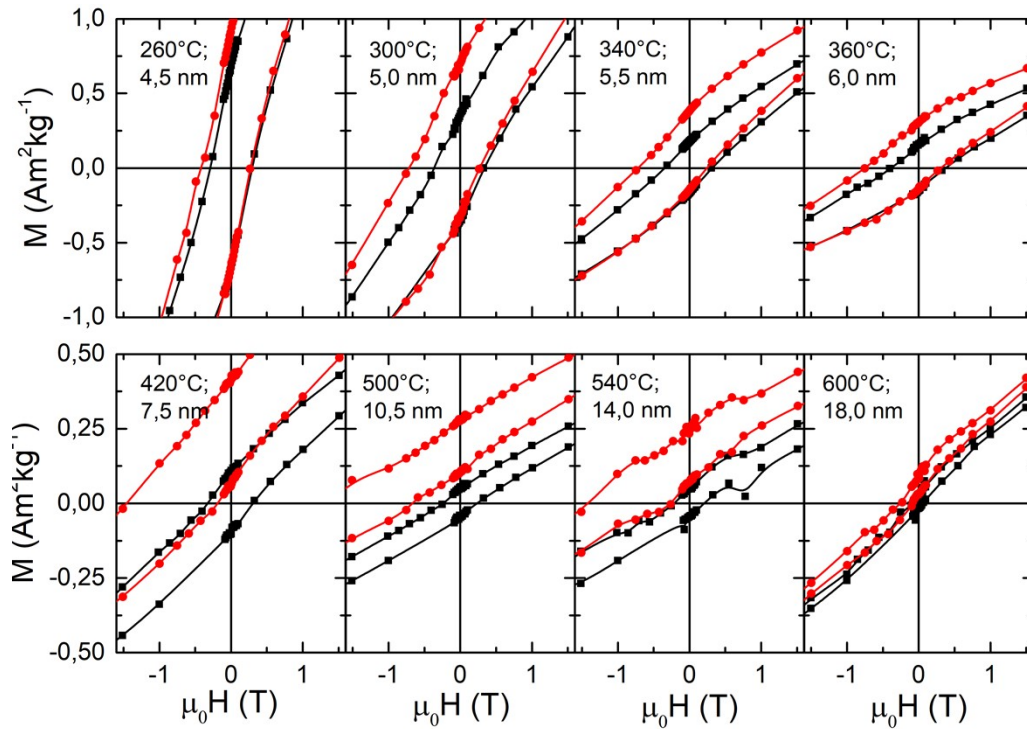


Figure S4: Zooms on the 5 K $M(H)$ loops of the NiO samples in ZFC (black) and FC (red) modes.

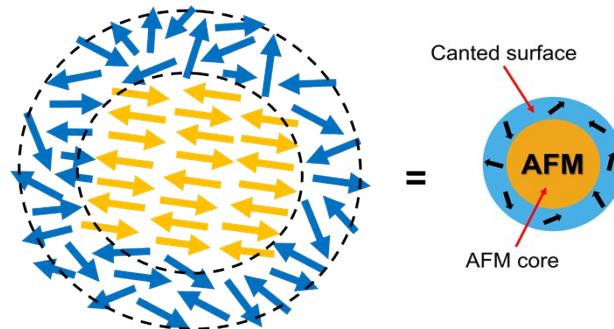


Figure S5: Schematic representation of the AFM core structure of NiO particles and their spin disordered surface shell

References

- [1] L. Poul, N. Jouini and F. Fiévet. 'Layered Hydroxide Metal Acetates (Metal = Zinc, Cobalt, and Nickel): Elaboration via Hydrolysis in Polyol Medium and Comparative Study'. *Chem. Mater.* vol. 12, no. 13, pp. 3123–3132 (2000).
- [2] D. S. Hall, D. J. Lockwood, C. Bock, B. R. Macdougall and D. J. Lockwood. 'Nickel hydroxides and related materials: a review of their structure, synthesis and properties'. *Proc. R. Soc. A* vol. 471, no. 2174, pp. 20140792 (2015).
- [3] C. Moya, J. Ara and X. Batlle. 'Unraveling the Magnetic Properties of NiO Nanoparticles: From Synthesis to Nanostructure'. *Magnetism* vol. 4, no. 3, pp. 252–280 (2024).

